

# Chemisorption and Diffusion of Atomic Hydrogen in and on Cluster Models of Pd, Rh, and Bimetallic PdSn, RhSn, and RhZn Catalysts

Alain Rochefort,<sup>1a</sup> Jan Andzelm,<sup>1a</sup> Nino Russo,<sup>1b</sup> and Dennis R. Salahub<sup>\*1a</sup>

Contribution from the Département de chimie, Université de Montréal, C.P. 6128, Succursale A, Montréal, Québec, H3C 3J7, Canada, and the Dipartimento di Chimica, Università della Calabria, I-87030 Arcavacata di Rende, Cosenza, Italy. Received March 15, 1990

**Abstract:** Results of LCGTO-MCP-LSD (Linear Combination of Gaussian Type Orbitals-Model Core Potential-Local Spin Density) calculations are reported for chemisorption and for bulk and surface diffusion of atomic hydrogen on clusters simulating the (111) and (100) surfaces of pure transition metals (Pd and Rh) and bimetallic catalysts (PdSn, RhSn, and RhZn). The replacement of a Pd or Rh atom near the hydrogen atom by Sn decreases the binding energy for hydrogen adsorption. In particular, the decrease is most pronounced when the non-transition metal lies in the first surface layer (e.g. 3.8 eV (2.4 eV) for Pd (PdSn) and 4.1 eV (2.8 eV) for Rh (RhSn)) but is also significant when the non-transition metal is placed as a second neighbor (e.g. 3.8 eV (3.1 eV) for Pd(PdSn) and 4.1 eV (2.9 eV) for Rh(RhSn)). For Zn substitution the behavior is less regular, one case of an increase in binding energy has been found. The presence of Sn or Zn on the surface significantly increases the equilibrium bond distances (e.g. 1.76 Å for Pd<sub>3</sub>Pd vs 1.93 Å for Pd<sub>2</sub>SnPd) and decreases the hydrogen perpendicular vibrational frequencies (e.g. 1166 cm<sup>-1</sup> for Pd<sub>3</sub>Pd vs 988 cm<sup>-1</sup> for Pd<sub>2</sub>SnPd). The energy profile for diffusion of hydrogen into the bulk of Pd and PdSn clusters via the (111) surface is modified by the presence of Sn in the second coordination shell; the barrier increases. For the Pd<sub>13</sub>H cluster we find that the chemisorption site is 0.33 eV more stable than the octahedral bulk-like site (the experimental difference is 0.26 eV). The top of the diffusion barrier that lies in the triangular surface site is calculated to be 0.78 eV above the minimum. For Pd<sub>7</sub>Sn<sub>6</sub> the energy difference between the chemisorption and octahedral sites is 0.55 eV and the "entrance" diffusion barrier increases to 1.15 eV. The hydrogen surface diffusion has been calculated with the aim of explaining the nature of the second, high-temperature, desorption peak recently reported for RhSn/SiO<sub>2</sub> catalysts. Our results, obtained for the Rh<sub>8</sub>Sn<sub>3</sub>-H system, show that hydrogen diffusion in the tin region is clearly unfavored. A consistent pattern has emerged from the calculations; the proximity of tin to hydrogen leads to destabilization. This should affect the recombination process to form H<sub>2</sub>, and possible implications of this for catalysis are discussed.

The discovery, in recent years, of the superior catalytic properties of certain metal alloys (e.g. RhSn, PdSn, PtSn, NiAl, RuCu, etc.) has stimulated both fundamental and applied research, leading to interesting applications of these bimetallic compounds as catalysts for many industrial reactions.<sup>2</sup> The main advantages of metal-alloy catalysts over the monometallic systems are the higher activity, stability, and, especially, the greater selectivity. For these reasons, several bimetallic catalysts have been proposed and tested for a large series of chemical reactions. Despite these studies, the elementary mechanism for the improved performance is not well established and, at present, two different hypotheses have been proposed: the so-called "geometric" explanation<sup>3</sup> and "electronic effects".<sup>4</sup> Supporting the former is the fact that the surface composition of the metal alloys is different from that of the monometallic systems; in the geometric explanation the atoms of the second metal divide up the metal surface into small ensembles that are unable to catalyze the undesirable reactions (e.g. hydrogenolysis, formation of a carbonaceous residue, etc.). This geometric effect can also affect the size and concentration of clusters of active (transition-metal) atoms with the introduction of the second metal and hence also affect the rates of the desirable reactions that are catalyzed. The "electronic effects" explanation suggests that the electronic characteristics of the metal of the pure catalyst are modified by the presence of the second component. In these modified electronic properties lie the superior catalytic properties of the system. The two hypotheses are, of course, not completely independent, and it is possible to postulate that the change in catalytic properties of metal alloys can be explained with a combination of both.

At present, these possible mechanisms for understanding the improved catalytic effect of the metal-alloy systems are essentially based on empirical data from experimental work, but little theoretical analysis has been performed on this subject.<sup>5</sup> In this paper, we present the first quantum chemical study, based on local density functional theory, of the hydrogen interaction with PdSn, RhSn, and RhZn bimetallic catalysts. Although the hydrogen interaction is not the whole story of the bimetallic catalysts, hydrogen is extensively used to characterize the metal-alloy systems and the interaction of hydrogen with the surface is often of prime importance (e.g. in hydrogenation and dehydrogenation reactions<sup>6</sup>). In addition, many intriguing aspects of the metal-hydrogen couple have recently been uncovered: diffusion into the bulk,<sup>7</sup> spillover phenomena,<sup>8</sup> unusual photoemission,<sup>9</sup> and complex thermal desorption behavior.<sup>6c</sup> In particular, an intense second desorption peak has been observed at higher temperature in the hydrogen thermodesorption spectra of RhSn/SiO<sub>2</sub> catalysts.<sup>6c,e</sup>

The PdSn supported catalysts show<sup>6b</sup> a promoting effect on the dehydrogenation reactions for converting cyclohexanone into phenol, cyclohexylamine into aniline, cyclohexanone into benzene, and 2-propanol into acetone, whereas the Rh-Sn catalysts exhibit very good selectivity and high activity for the hydrogenation of

(5) Salahub, D. R.; Raatz, F. *Int. J. Quantum Chem.* **1984**, *S18*, 173.

(6) (a) Clarke, J. K. A.; Taylor, J. F. *J. Chem. Soc., Faraday Trans. 1* **1976**, 917. (b) Masai, M.; Honda, K.; Kubota, A.; Ohamaka, S.; Nishikawa, Y.; Nalchana, K.; Kishic, K.; Ikeda, S. *J. Catal.* **1977**, *50*, 419. (c) Candy, J.-P.; Ferretti, O. A.; Bournonville, J.-P.; Mabilon, G. *J. Chem. Soc., Chem. Commun.* **1985**, 1197. (d) Candy, J.-P.; El Mansour, A.; Ferretti, O. A.; Mabilon, G.; Bournonville, J.-P.; Basset, J. M.; Martino, G. *J. Catal.* **1988**, *112*, 201. (e) Candy, J.-P.; Ferretti, O. A.; Mabilon, G.; Bournonville, J.-P.; El Mansour, A.; Basset, J. M.; Martino, G. *J. Catal.* **1988**, *112*, 210.

(7) Andzelm, J.; Salahub, D. R. In *Physics and Chemistry of Small Clusters*; Jena, P., Rao, B. K., Khanna, S., Eds.; NATO ASI Ser. E, **1987**, Vol. 158, p 867 and reference therein.

(8) King, T. S.; Wu, X.; Gerstein, B. C. *J. Am. Chem. Soc.* **1986**, *108*, 6056.

(9) Eberhardt, W.; Louie, S. G.; Plummer, E. W. *Phys. Rev. B* **1983**, *28*, 465.

(1) (a) Université de Montréal. Current address for J.A.: Cray Research Inc., 655-E Lone Oak Drive, Eagan, Minnesota 55120. Current address for A.R.: Institut Français du Pétrole, B.P. 311, 92506 Rueil Malmaison Cédex, France. (b) Università della Calabria.

(2) Sinfelt, J. H. *Bimetallic Catalysts—Discoveries, Concepts and Applications*; Wiley: New York, 1983.

(3) Ponc, Y. *Prog. Surf. Membr. Sci.* **1979**, *13*, 1.

(4) Verbeek, H.; Sachtler, W. M. H. *J. Catal.* **1976**, *42*, 257.

ethyl acetate into ethanol.<sup>6d</sup> Alloys involving Zn have been studied less;<sup>10</sup> however, they are receiving increasing attention<sup>9</sup> for reactions such as the hydroformylation of ethylene.<sup>10a</sup> We have made calculations for RhZn in order to have at least some indication of whether the effects discovered for Sn are specific to that metal and whether some "tuning" ability might be achieved through varying the non-transition metal.

Our study involves a variety of cluster models for PdSn, RhSn, and RhZn bimetallic catalysts, chosen to sample possible environments of hydrogen chemisorbed on the surface, diffusing across it, or diffusing into the bulk. An important feature of the study is that both thermodynamic and kinetic aspects have been considered. We have found a general effect of the substitution of Sn for Pd or Rh on the metal-hydrogen interaction. The binding is weakened and this can be traced to the occupation (or lack of emptying) of orbitals of Sn-H antibonding character. Similar interactions are responsible for increased barriers to surface and bulk diffusion. The decreased mobility of hydrogen atoms "activated" on tin-rich areas of the catalyst may be an important component of the catalytic mechanisms.

## Method

The LCGTO-MCP-LSD (Linear Combination of Gaussian Type Orbitals-Model Core Potential-Local Spin Density) method employed has been described extensively elsewhere.<sup>11</sup> It is a self-consistent-model core-potential scheme utilizing a local density description of the exchange and correlation potential and energy. The VWN<sup>12</sup> potential, which is thought to represent the LSD limit, has been used. For the fitting of the density and exchange-correlation potential, the auxiliary basis set, calculated with use of our fitting procedure,<sup>11b</sup> has been used. For Pd and Rh we have used an extended (Pd<sup>16+</sup>, Rh<sup>15+</sup>) model core potential<sup>13a,b</sup> that allows the explicit treatment of 5s, 5p, 4d, and the "semicore" 4p electrons in cluster calculations. For Sn, the Sn<sup>14+</sup> MCP is that recently presented<sup>13c</sup> in which only the 5s and 5p electrons are in the valence shell. Finally, for the Zn atom, a Zn<sup>12+</sup> MCP with valence 4s, 4p, and 3d electrons has been employed. For all the MCP, the effect of scalar relativity has been taken into account. The valence-electron basis sets, in a short notation for the contraction pattern, are (2211/2111\*/121) for Pd and Rh, (2111/211/211) for Zn, and (2211/211/1\*) for Sn. The corresponding auxiliary basis sets are (734/734) for Pd and Rh, (634/634) for Zn, and (734/733) for Sn. For hydrogen a (5s) orbital set was contracted to the [2s] level and augmented with a p polarization function with exponent 0.5, to yield a (41/1\*) set. The corresponding auxiliary basis set is (511/411). Exponents and contraction coefficients are available on request.

The spectroscopic constants were calculated by fitting the potential curve with third-degree polynomials and the binding energies were derived by using the interpolated total energies. The basis set superposition error (BSSE) has been calculated as described in ref 11b. Because of the high quality of our basis sets the BSSE was found to have only a small influence on the calculated properties, well within the inherent uncertainties of the cluster models and of the LSD hamiltonian.

For the bare Pd and Rh clusters, the experimental geometry of the bulk fcc crystals was used. Since the structure of the alloys is unknown, we have used the same geometry also for the mixed clusters. In this approximation, the Sn or Zn atom is simply substituted for the transition-metal atom. However, we have considered the possible influence of the replacement of palladium by tin on the surface properties, by considering the geometric relaxation of small, four-atom, pure Pd or mixed PdSn clusters. The results (see next section) show that this does not affect the significant features of the interactions and we have therefore used the unrelaxed surface for all the other calculations. Finally, as further tests for the MCPs, we have performed both spin-polarized and unpolarized calculations for the SnH and ZnH molecules in their ground states (<sup>2</sup>Π and <sup>2</sup>Σ for SnH and ZnH, respectively). For SnH, the

**Table I.** Structural and Spectroscopic Parameters (Corrected for BSSE) for Hydrogen Chemisorption on the Three- and Fourfold Site of Pd, Rh, PdSn, and RhSn and on the Threefold Site of Sn, Zn, and RhZn Clusters (See Figure 1)

| clusters   | $r_{\perp}$ /Å | $R_e$ /Å | $\omega_e$ /cm <sup>-1</sup> | $D_e$ /eV |
|--|----------------|----------|------------------------------|-----------|
| (111)  |                |          |                              |           |
| H-Pd <sub>3</sub> (3)  | 0.79           | 1.78     | 815                          | 4.3       |
| H-Pd <sub>3</sub> Pd (3,1)   | 0.79           | 1.78     | 1166                         | 3.8       |
| H-Pd <sub>3</sub> Sn (3,1)   | 0.83           | 1.78     | 1184                         | 3.1       |
| H-Pd <sub>2</sub> SnPd (3,1)   | 1.08           | 1.92     | 988                          | 2.4       |
| H-Sn <sub>3</sub> Sn (3,1) <sup>b</sup>                                    | 1.36           | 2.09     | 1067                         | 2.2       |
| H-Pd <sub>2</sub> Pd <sub>2</sub> Pd (6,6,1)                               | 0.92           | 1.79     | 1113                         | 3.4       |
| H-Pd <sub>2</sub> Sn <sub>2</sub> Pd (6,6,1)                               | 1.01           | 1.92     | 1173                         | 3.2       |
| H-Pd <sub>2</sub> Pd <sub>2</sub> PdPd <sub>3</sub> (6,6,1,3) <sup>c</sup> | 0.90           | 1.79     | 1101                         | 3.3       |
| H-Rh <sub>3</sub> Rh (3,1)   | 0.99           | 1.84     | 1439                         | 4.1       |
| H-Rh <sub>3</sub> Sn (3,1)   | 0.90           | 1.80     | 1304                         | 2.9       |
| H-Rh <sub>2</sub> SnRh (3,1)   | 1.10           | 1.90     | 1224                         | 2.8       |
| H-Sn <sub>3</sub> Sn (3,1)   | 1.40           | 2.09     | 1096                         | 2.8       |
| H-Rh <sub>3</sub> Rh <sub>3</sub> Rh (3,3,1)                               | 0.94           | 1.82     | 1362                         | 4.4       |
| H-Rh <sub>3</sub> Sn <sub>3</sub> Rh (3,3,1)                               | 0.82           | 1.76     | 993                          | 3.6       |
| H-Rh <sub>3</sub> Zn (3,1)   | 0.91           | 1.80     | 1311                         | 4.8       |
| H-Rh <sub>2</sub> ZnRh (3,1)   | 0.90           | 1.79     | 1308                         | 3.4       |
| H-Zn <sub>3</sub> Zn (3,1) <sup>d</sup>                                    | 0.94           | 1.82     | 848                          | 1.1       |
| (100)  |                |          |                              |           |
| H-Pd <sub>4</sub> Pd <sub>5</sub> (4,5)                                    | 0.08           | 1.95     | 669                          | 3.3       |
| H-Pd <sub>4</sub> PdSn <sub>4</sub> (4,5)                                  | 0.13           | 1.96     | 883                          | 3.0       |
| H-Rh <sub>4</sub> Rh <sub>5</sub> Rh <sub>4</sub> (4,5,4)                  | 0.63           | 2.00     | 781                          | 3.7       |
| H-Rh <sub>4</sub> Rh <sub>5</sub> Sn <sub>4</sub> (4,5,4)                  | 0.51           | 1.97     | 812                          | 3.7       |

<sup>a</sup> Experimental values for the H/Pd(111) surface are  $R_e = 1.69$  Å,  $\omega_e = 998$  cm<sup>-1</sup>, and  $D_e = 2.7$  eV. Experimental values for the H/Pd-(100) surface are  $\omega_e = 511$  cm<sup>-1</sup> and  $D_e = 2.8$  eV. Experimental values for the H/Rh(111) surface are  $\omega_e = 740$  or 1100 or 1410 cm<sup>-1</sup> and  $D_e = 2.05$  eV. Experimental values for the H/Rh(100) surface are  $d_{\perp} = 0.8$  Å,  $\omega_e = 685$  or 1031 or 1136 cm<sup>-1</sup>, and  $D_e = 2.65$  eV. <sup>b</sup> Lattice parameter of Pd. <sup>c</sup> Without BSSE correction. <sup>d</sup> Lattice parameter of Rh.

equilibrium distance is found to be 1.775 Å in both types of calculations. The corresponding experimental value is 1.781 Å for <sup>120</sup>SnH and 1.771 Å for <sup>120</sup>Sn<sup>2</sup>H. The calculated vibrational frequency is 1204 and 1202 cm<sup>-1</sup> at unpolarized and spin-polarized levels, respectively, whereas the experimental value is 1188 cm<sup>-1</sup>. The spin-polarized binding energy is 2.99 eV (2.72 eV, unpolarized) vs ≤2.73 eV (experimental). For ZnH, we find a (spin-polarized) equilibrium distance of 1.590 Å and a vibrational frequency of 1611 cm<sup>-1</sup>. The binding energy is found to be 1.2 eV. The corresponding experimental values<sup>14</sup> are 1.600 Å, 1608 cm<sup>-1</sup>, and 0.9 eV, respectively. The agreement between our values and experiment is excellent as it was for the PdH molecule.<sup>13a</sup>

## Results and Discussion

**Surface Relaxation.** As a first step, we have considered whether the relaxation of the surface of the simplest clusters is appreciable and how this is affected by Sn replacement. For this purpose, we have chosen to study the case of palladium, specifically the Pd<sub>4</sub> cluster shown in Figure 1. We have optimized the distance between the two layers of the cluster, the optimized distance (1.892 Å) being not too different from the unrelaxed value (1.951 Å). When the Pd atom of the second layer is replaced by Sn we found an optimum interlayer spacing of 2.007 Å, about 0.06 Å larger than the bulk palladium value. These results indicate that there is unlikely to be a drastic change in geometry, either between small clusters and the bulk or as a result of alloying (in fact the two effects will tend to cancel to some extent). In view of these results, and considering the enormous computational complexity associated with geometry variation, especially of larger clusters, we have chosen to keep the cluster geometries fixed at those of the bulk transition metal. Past work on chemisorption on ideal clusters of palladium and rhodium has largely demonstrated that this approximation is reasonable for a first description of the chemisorption and diffusion properties.<sup>7,13a</sup> Of course, quantitative treatments of adsorbate structure, vibrations, and diffusion will

(10) (a) Ichikawa, M.; Lang, A. J.; Shriver, D. F.; Sachtler, W. M. H. *J. Am. Chem. Soc.* **1985**, *107*, 7216. (b) Jen, H. W.; Zheng, Y.; Shriver, D. F.; Sachtler, W. M. H. *J. Catal.* **1989**, *116*, 361.

(11) (a) Dunlap, B. J.; Connolly, J. W. D.; Sabin, J. R. *J. Chem. Phys.* **1979**, *71*, 3396, 4993. (b) Andzelm, J.; Radzio, E.; Salahub, D. R. *J. Chem. Phys.* **1985**, *83*, 4573. (c) Salahub, D. R. *Adv. Chem. Phys.* **1987**, *69*, 447.

(12) Vosko, S. H.; Wilk, L.; Nusair, N. *Can. J. Phys.* **1980**, *58*, 1200.

(13) (a) For Pd see: Andzelm, J.; Salahub, D. R. *Int. J. Quantum Chem.* **1986**, *29*, 1091. (b) For Rh see: Russo, N.; Andzelm, J.; Salahub, D. R. *Chem. Phys.* **1987**, *114*, 331. (c) For Sn see: Andzelm, J.; Russo, N.; Salahub, D. R. *J. Chem. Phys.* **1987**, *87*, 6562. (d) For Zn see: Rocheffort, A. M. Sc. Thesis, Université de Montréal 1989.

(14) Huber, H. P.; Herzberg, G. *Molecular Spectra and Molecular Structure. Constants of Diatomic Molecules*; Van Nostrand Reinhold: New York, 1979; Vol. 4.

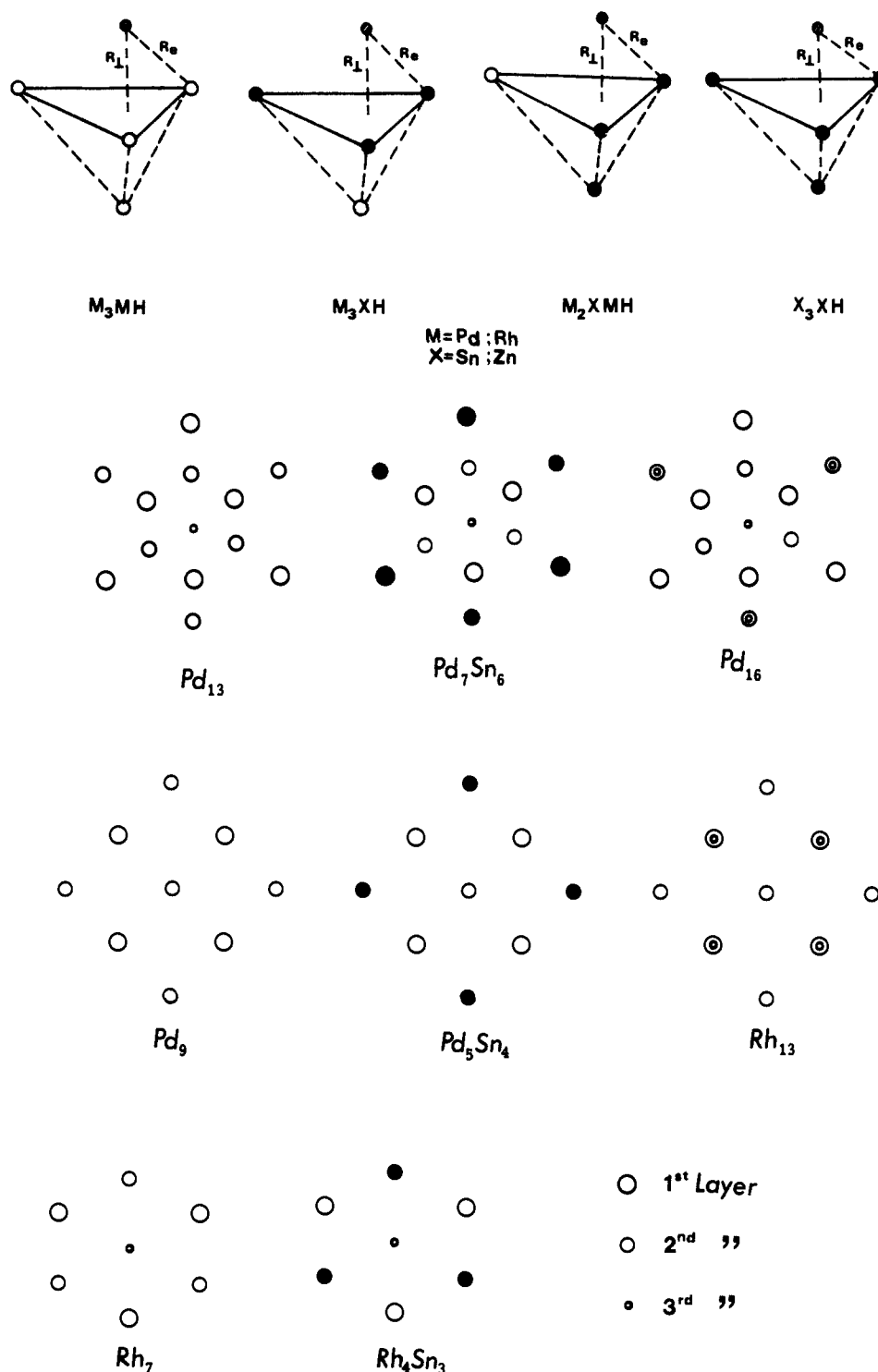


Figure 1. Structures of the clusters studied. Circles of decreasing size represent atoms in successively deeper layers.

often require consideration of surface relaxation and of surface vibrations (see, for example, the recent work of the Truhlar<sup>15a</sup> and DePristo<sup>15b</sup> groups on surface diffusion). It is likely that in the not too distant future such questions can be reopened, once the calculation of analytic gradients<sup>16</sup> and associated optimization routines<sup>17</sup> become more fully established. However, we believe

the trends and concepts that have been isolated from our calculations transcend the quantitative details and are sufficiently strong to remain valid in the presence of relaxation and lattice dynamic effects (see further below).

**Hydrogen Chemisorption.** Since the preferred chemisorption sites of hydrogen on Pd and Rh (111) and (100) surfaces are well established to be the 3-fold and 4-fold sites,<sup>18</sup> respectively, we have

(15) (a) Truong, T. N.; Truhlar, D. G. *J. Chem. Phys.* **1988**, *88*, 6611 and references therein. (b) Kara, A.; DePristo, A. E. *J. Chem. Phys.* **1990**, *92*, 5653.

(16) Fournier, R.; Andzelm, J.; Salahub, D. R. *J. Chem. Phys.* **1989**, *90*, 6371.

(17) (a) St-Amant, A. G.; Salahub, D. R. *Chem. Phys. Lett.* **1990**, *169*, 387. (b) St-Amant, A. G.; Papai, I.; Ushio, J.; Salahub, D. R. *Int. J. Quantum Chem.* In press. (c) St-Amant, A. G.; Godbout, N.; Salahub, D. R. Unpublished.

(18) (a) Eberhardt, W.; Greuter, F.; Plummer, E. W. *Phys. Rev. B* **1983**, *28*, 465; *Phys. Rev. Lett.* **1981**, *48*, 1085. (b) Conrad, H.; Ertl, G.; Latta, E. *Surf. Sci.* **1974**, *41*, 435. (c) Conrad, H.; Kordes, M. E.; Steuzel, R. W. *J. Electron Spectrosc. Rel. Phenomena* **1986**, *38*, 289. (d) Nyberg, C.; Tengstal, C. G. *Phys. Rev. Lett.* **1983**, *50*, 1680. (e) Behm, R. J.; Christmann, K.; Ertl, G. *Surf. Sci.* **1980**, *99*, 320. (f) Christmann, K. *Surf. Sci. Rep.* **1988**, *9*, 1. (g) Ehsasi, M.; Christmann, K. *Surf. Sci.* **1988**, *194*, 172. (h) Richter, L. J.; Ho, W. *J. Vac. Sci. Technol.* **1987**, *A5*, 453.

investigated the interaction of H with these sites. In Table I we have collected the most important parameters derived from the calculations. To test the sensitivity of the calculated properties to cluster size, for the case of pure Pd(111) models we have examined clusters containing from 4 to 16 atoms. The results show that the equilibrium distance and the vibrational frequency are not very size-dependent. The binding energy decreases somewhat, toward the experimental heat of chemisorption of 2.6 eV for Pd(111),<sup>18b</sup> as the cluster size increases, but the effect is much less dramatic than for, say, the case of CO adsorption on Pd.<sup>19</sup> This can perhaps be taken as support for the idea of Norskov<sup>20</sup> that the hydrogen binding is relatively simple and that the hydrogen atom can find an "ideal" environment on a surface by (slightly) changing its position. Indeed, we also find that the binding energies for chemisorption on corresponding Pd and Rh clusters while different (the binding to rhodium is slightly stronger) are not dramatically so. However, we differ from Norskov in the remainder of the interpretation. In our calculations (see below), the role of the d electrons is paramount.

A referee has raised the question of why the convergence of the binding energy with cluster size is relatively rapid and smooth, whereas Hartree-Fock (and contracted configuration interaction) calculations yield a much more erratic behavior.<sup>21</sup> The "cure" proposed for this in the Hartree-Fock approach was to calculate binding energies with reference to an excited state of the cluster which is "prepared" for interaction with the adsorbate (for example, in the case of H adsorption, a cluster state with a singly occupied totally symmetric orbital), the reasoning being that for an extended surface such an orbital should be available near the Fermi level. We believe that the differing behavior of the density functional and Hartree-Fock methods can ultimately be traced to different treatments of the virtual orbitals in the two cases. As is well-known, in HF the virtual orbitals are determined in the field of  $N$  electrons rather than the physically correct  $N - 1$  electron field and, hence, lie too high. For the case of an infinite metal, this is ultimately related to a pathological behavior of the HF method, which is well-known among solid-state physicists, namely, that the HF density of states vanishes at the Fermi level.<sup>22</sup> To recover metallic behavior within this approach would then require massive correlation corrections. On the other hand, in the local density functional approach the occupied and virtual levels are all determined from the same operator and metallic behavior arises naturally in the infinite limit. For small metal clusters the gap between occupied and virtual levels is smaller in LDF than in the HF approach and, indeed, quite "bulk-like" densities of states have been generated for a number of metals by broadening the energy level diagram for small clusters.<sup>23</sup> So, in a manner of speaking, the LDF clusters are already "prepared" for binding in the sense proposed by Siegbahn.<sup>21a</sup> In the final analysis, in our view, the erratic convergence observed in the traditional *ab initio* approaches is a manifestation not so much of a real cluster size effect but, rather, of correlation effects which, in turn, are highly sensitive to the cluster size when treated by the usual HF-based approach.

Returning to Table I, the results for Pd<sub>13</sub>H may be compared with experimental values for the bulk palladium surface and with the results of slab calculations. Our calculated equilibrium distance is 1.79 Å, which may be compared with that (1.69 Å) proposed on the basis of a comparison of photoemission data with local density slab calculations,<sup>9</sup> and with a pseudopotential CI value of 1.72 Å for a Pd<sub>3</sub> cluster.<sup>24</sup> In addition, our value is consistent

with the value of 1.78 Å derived from previous LSD calculations on Pd<sub>10</sub>H.<sup>25</sup> Concerning the vibrational frequency we found a value of 1166 cm<sup>-1</sup> for the smallest cluster, Pd<sub>3</sub>, and 1133 cm<sup>-1</sup> for Pd<sub>13</sub>. The experimental value is reported as 998 cm<sup>-1</sup>.<sup>18c</sup>

For chemisorption on the Pd(100) surface we have used a Pd<sub>3</sub> cluster (Figure 1). The hydrogen lies at 0.08 Å above the surface with a Pd-H distance of 1.95 Å and the vibrational frequency is 699 cm<sup>-1</sup>. The experimental frequency for H adsorbed on the 4-fold site of Pd(100) is 511 cm<sup>-1</sup>. For the binding energy, the value for Pd<sub>3</sub>H (3.3 eV) is above, but not too far from the experimental heat of chemisorption (2.8 eV for Pd(100))<sup>18e</sup>. In addition to the cluster size error, the difference also reflects the usual overbinding of the LSD hamiltonian, when nonlocal corrections are not taken into account.<sup>11c</sup> In view of the relative insensitivity of the spectroscopic parameters to cluster size for palladium, we have limited our attention for the rhodium clusters to the "minimum", 4-atom, case plus a medium-sized, 7-atom cluster for the (111) surface and a Rh<sub>13</sub>H one for the (100) surface. Also for these systems, the results are in good agreement with available experimental results.<sup>18</sup>

Turning now to the alloys, we start with a 4-atom model. As mentioned in the preceding section, because the chemical and structural composition of the chemisorption sites for PdSn, RhSn, and RhZn alloy catalysts are not known, we have considered two clusters with different positions of Sn or Zn. In the first, M<sub>3</sub>Sn(Zn), the Sn(Zn) lies in the second layer so that the H...Sn(Zn) interaction is "indirect". In the second, M<sub>2</sub>Sn(Zn)M, since the Sn(Zn) lies in the surface layer, a direct interaction is allowed (Figure 1). In the case of indirect H...Sn(Zn) contact, all the calculated properties remain essentially unchanged, with the exception of the binding energy. In all cases, for Sn substitution, the binding energy undergoes a considerable decrease with respect to the pure Pd or Rh cluster. This is also true for the case of Zn substitution in the top layer, but in the case of replacement in the second layer there is a binding energy increase, in the presence of zinc. This difference between tin and zinc might possibly be of use in "tuning" catalysts, but we will not dwell on this here.

For the case of M<sub>2</sub>SnMH all of the properties undergo clear systematic changes that can be attributed to the H...Sn contact. For the PdSn case, the perpendicular H-surface distance increases by 0.3 Å, the Pd-H distance increases by 0.14 Å, the vibrational frequency decreases by about 200 cm<sup>-1</sup>, and the binding energy decreases by 1.4 eV. Similar changes are observed for the rhodium analogue. For the case of Rh<sub>2</sub>ZnRhH, there is a similar trend for the vibrational frequency and for the bond energy but the bond distance actually decreases a little. For the purposes of comparison we have also investigated the chemisorption of H on pure Sn and Zn clusters, with the geometry of the transition metals. In addition to a further elongation of the bond length, we note that the binding energy is much lower, both on Sn and on Zn, than on either the pure transition-metal clusters or the alloys.

At this point we have extended our investigation to larger clusters for both the (111) and (100) surfaces and have considered the effect of "indirect" interactions. Such indirect interactions widen the variety of adsorption sites and provide information on the range of the alloying effects. We have focused our chemisorption studies on Pd and Rh in a "field" of tin atoms. Returning to Table I, we note, comparing Pd<sub>13</sub>H with Pd<sub>7</sub>Sn<sub>6</sub>H, that the presence of tin causes the equilibrium distance to increase and the binding energy to decrease, as was the case for the smaller clusters. There is a slight increase in vibrational frequency, but we are not sure it is significant; the estimated errors due to curve fitting are probably several tens of wavenumbers. The clusters simulating the (111) surface of rhodium or the (100) surface of palladium also show small shifts in bond distances and frequencies,

(19) Andzelm, J.; Salahub, D. R. *Int. J. Quantum Chem.* **1986**, *29*, 1091.

(20) Norskov, J. K.; Besenbacher, F. J. *Less Common Metals* **1987**, *30*, 475; Nordlander, P.; Norskov, J. K.; Besenbacher, F. *J. Phys. F* **1986**, *16*, 1161.

(21) (a) Panas, I.; Schüle, J.; Siegbahn, P.; Wahlgren, U. *Chem. Phys. Lett.* **1988**, *149*, 265. (b) Hermann, K.; Bagus, P. S.; Nelin, C. J. *Phys. Rev. B* **1987**, *35*, 9467.

(22) Monkhorst, H. *Phys. Rev. B* **1979**, *20*, 1504.

(23) (a) Salahub, D. R.; Messmer, R. P. *Phys. Rev. B* **1977**, *16*, 2526. (b) Yang, C. Y.; Johnson, K. H.; Salahub, D. R.; Kaspar, J.; Messmer, R. P. *Phys. Rev. B* **1981**, *24*, 5673.

(24) Pacchioni, G.; Koutecky, J. *Surf. Sci.* **1985**, *154*, 126.

(25) (a) Baykara, N. A.; Andzelm, J.; Salahub, D. R.; Baykara, S. Z. *Int. J. Quantum Chem.* **1986**, *29*, 1025. (b) A. Peluso and D. R. Salahub, unpublished. The energies for HPd<sub>10</sub> of ref 21a should be replaced by 0.0 eV (CHEM), 0.79 eV (TRI ENT), 0.40 eV (OCT), 0.97 eV (TRI INT), and 0.53 eV (TET).

(26) Schlapbach, L.; Burger, J. P. *J. Phys. Lett.* **1982**, *43*, L273.

(27) Kubiak, G. D.; Stulen, R. H. *J. Vac. Sci. Technol.* **1986**, *A4*, 1427.

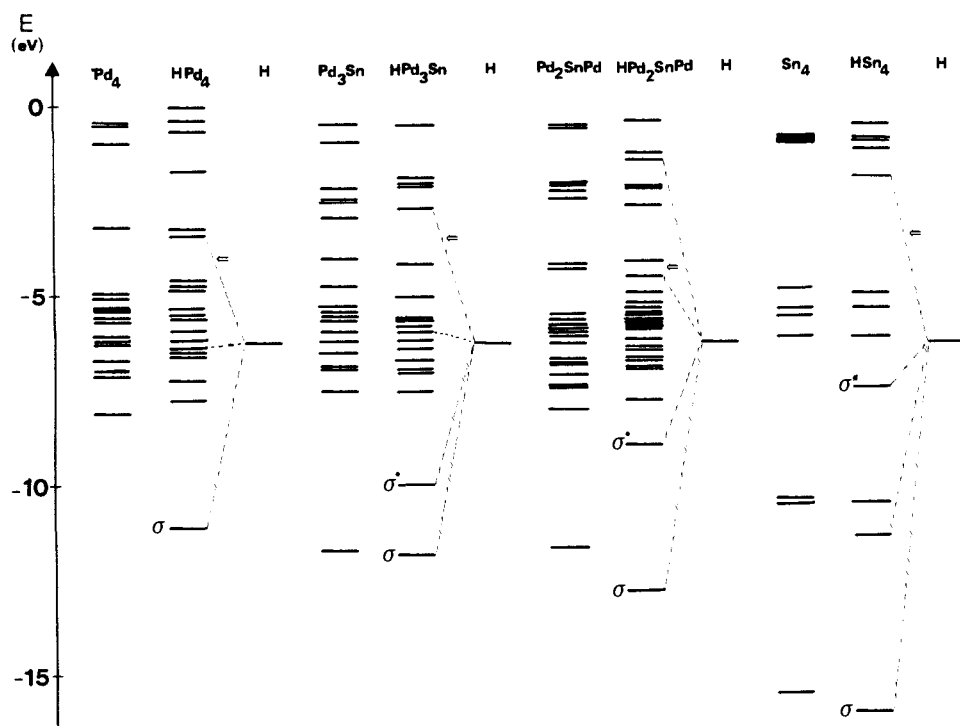


Figure 2. Orbital energies for the interaction of atomic hydrogen with (a) Pd<sub>4</sub>, (b) Pd<sub>3</sub>Sn, (c) Pd<sub>2</sub>SnPd, and (d) Sn<sub>4</sub>.

in one direction or the other, when Sn is in the second coordination shell. Of most importance for what follows, however, is that the presence of tin systematically decreases the binding energy. In order to put limits on the range of such indirect effects we have made calculations for a Rh<sub>13</sub>H cluster and for its analogue in which four tin atoms are placed in the third layer. All of the chemisorption properties are virtually unchanged from their values for the pure transition-metal cluster.

The systematic decrease of hydrogen binding energy, strongest when the tin atoms lie in the surface but still appreciable out to second neighbor positions, could have immediate consequences for the catalysis of these systems. (Note that for the RhZn alloys the result depends sensitively on the position of the zinc atom.) The hydrogen is less tightly bound, and this could make it more accessible for certain types of reactions. We have not performed any calculations for the "other" partner in a reaction but it is to be expected that alloying may have equally important consequences for these (in addition to ensemble effects, etc. for large molecules).

The above finding, the decrease in the binding energy, also raises a dilemma, however. There has been a recent report of thermal desorption spectra for RhSn/SiO<sub>2</sub> catalysts<sup>6c,e</sup> and these show, in addition to the peak at relatively low temperature (~400 K) corresponding to desorption from "pure" transition metal, a second peak at high temperature (~800 K). A naive interpretation would attribute this to *more* tightly bound hydrogen in the presence of tin, rather than the result we find of weaker binding. Before returning to this question, we pause to describe the binding between hydrogen and the clusters and to offer an orbital explanation for the decreased binding energy.

**Description of the Binding.** The decrease in the interaction energy in the presence of the non-transition metal can be rationalized with reference to the orbital energy diagram and Mulliken population analysis for the studied systems. In Figure 2, the orbital energy diagrams for HPd<sub>4</sub>, HPd<sub>3</sub>Sn, HPd<sub>2</sub>SnPd, and HSn<sub>4</sub> are reported, and in Table II the corresponding Mulliken population analyses of the levels are given. In Table III are reported the corresponding orbital compositions for RhSn systems, and Figure 3 shows the orbital energies for Zn alloys.

H interacting with Pd<sub>4</sub> leads to the well-known split-off state below the d band (at -11.1 eV).<sup>9</sup> This level has 52% H(s) character and 42% Pd(d) character. The contour diagram shown in Figure 4a reveals its bonding character. Another level, within

Table II. Composition (%) of Molecular Orbitals of HPd<sub>4</sub> and Different HPd<sub>4-n</sub>Sn<sub>n</sub> and HSn<sub>4</sub> Clusters

| level<br>-ε, eV       | H<br>1s | Sn |    | Pd |    |    | nature |
|-----------------------|---------|----|----|----|----|----|--------|
|                       |         | 5s | 5p | 5s | 5p | 4d |        |
| HPd <sub>4</sub>      |         |    |    |    |    |    |        |
| 11.1                  | 52      |    |    | 3  | 3  | 42 | σ      |
| 6.4                   | 8       |    |    | 40 | 1  | 51 | σ*     |
| 3.4                   | 16      |    |    | 84 | 0  | 0  | σ*     |
| HPd <sub>3</sub> Sn   |         |    |    |    |    |    |        |
| 11.8                  | 5       | 63 | 2  | 10 | 10 | 10 | σ      |
| 10.7                  | 45      | 13 | 0  | 0  | 1  | 41 | σ*     |
| 6.0                   | 10      | 6  | 22 | 22 | 0  | 40 | σ*     |
| 2.8                   | 23      | 0  | 46 | 1  | 12 | 18 | σ*     |
| HPd <sub>2</sub> SnPd |         |    |    |    |    |    |        |
| 12.8                  | 21      | 56 | 6  | 3  | 2  | 12 | σ      |
| 9.0                   | 26      | 22 | 7  | 5  | 1  | 39 | σ*     |
| 4.6                   | 10      | 0  | 16 | 49 | 0  | 25 | σ*     |
| 1.4                   | 17      | 0  | 26 | 14 | 43 | 0  | σ*     |
| HSn <sub>4</sub>      |         |    |    |    |    |    |        |
| 16.0                  | 7       | 73 | 20 |    |    |    | σ      |
| 11.4                  | 19      | 60 | 21 |    |    |    | σ*     |
| 7.5                   | 29      | 45 | 26 |    |    |    | σ*     |
| 2.0                   | 35      | 0  | 65 |    |    |    | σ*     |

the d band at -6.4 eV, has about 10% H(s), 51% Pd(d), and 40% Pd(s) character. It shows (Figure 4b) both bonding and antibonding H-Pd interactions and is probably best characterized as nonbonding. The strongly antibonding Pd-H levels (the lowest lie at -3.4 eV) are above the Fermi energy and therefore empty, leading to net strong bonding.

When one of the Pd atoms in the first layer is replaced by Sn, two "split-off" states result as well as a "nonbonding" level at -4.6 eV, similar to that just discussed for HPd<sub>4</sub> (see Figure 2c). The lowest split-off state is composed of 21% H(s), 12% Pd(d), and 56% Sn(s). This level is bonding with respect to both Pd-H and Sn-H (Figure 3c). The other "split-off" level, at -9.0 eV, has a weight of 26% on H(s), 32% on Pd(d), and 22% on Sn(s). It is Pd-H bonding but Sn-H *antibonding*. This occupied antibonding level is clearly consistent with the decreased binding energy. One can perhaps view this aspect of the electronic structure as arising from the strong Pd(d)-H interactions that determine the energy range of the split-off states. The weaker

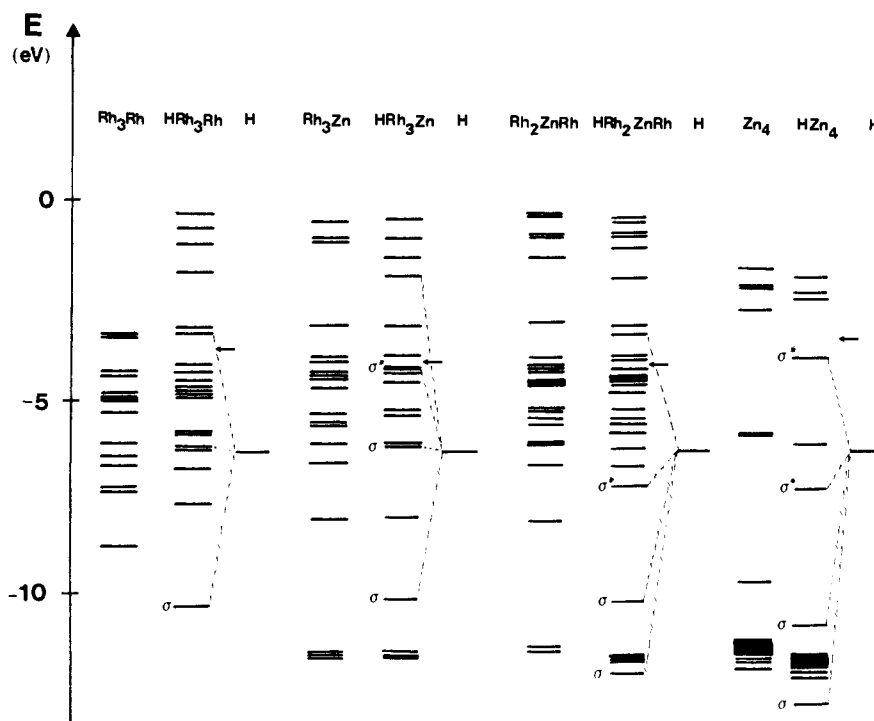


Figure 3. Orbital energies for the interaction of atomic hydrogen with (a)  $Rh_4$ , (b)  $Rh_3Zn$ , (c)  $Rh_2ZnRh$ , and (d)  $Zn_4$ .

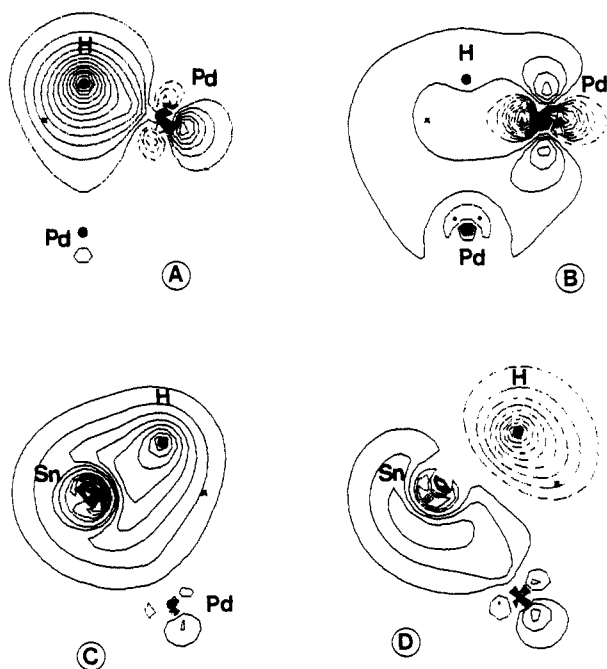


Figure 4. Orbital wave functions for (a) the level at  $-11.1$  eV of  $HPd_4$ , (b) the level at  $-6.4$  eV of  $HPd_4$ , (c) the level at  $-12.8$  eV of  $HPd_2SnPd$  and (d) the level at  $-9.0$  eV of  $HPd_2SnPd$ .

Sn-H interaction leads to a small bonding-antibonding splitting, insufficient to push the Sn-H antibonding level above  $E_F$  and empty it.

The presence of tin in the second layer has qualitatively the same effect. In this case the two "split-off" states lie at  $-1.8$  and  $-10.7$  eV, respectively (Figure 2b), and the first has a lower H(s) character (5%) and a higher Sn(s) contribution (63%). The Pd(d) contribution is unchanged. The second is shifted to  $-10.7$  eV and the H(s) and Sn(s) components become 45% and 13%, respectively, whereas the Pd(d) component does not change in this case either. The nonbonding level is now at  $-6.0$  eV (remaining under  $E_F$  as in the case of the  $HPd_4$  cluster). Finally, if we analyze the electronic levels for the interaction of hydrogen with the pure  $Sn_4$  cluster (Figure 2d), we see that the bonding level of  $HPd_4$  has

Table III. Composition (%) of Molecular Orbitals of  $HRh_4$  and  $HRh_{4-n}Sn_n$  and  $HRh_{4-n}Zn_n$  Clusters

| level<br>$-\epsilon$ , eV     | H<br>1s | Sn |    |    | Rh |    |    | nature     |
|-------------------------------|---------|----|----|----|----|----|----|------------|
|                               |         | 5s | 5p | 5s | 5p | 4d |    |            |
| <b><math>HRh_4</math></b>     |         |    |    |    |    |    |    |            |
| 10.3                          | 47      |    |    | 20 | 0  | 33 |    | $\sigma$   |
| 6.1                           | 6       |    |    | 39 | 0  | 55 |    | $\sigma^*$ |
| 3.4                           | 12      |    |    | 12 | 43 | 33 |    | $\sigma^*$ |
| <b><math>HRh_3Sn</math></b>   |         |    |    |    |    |    |    |            |
| 11.8                          | 10      | 73 | 4  | 4  | 0  | 9  |    | $\sigma$   |
| 10.8                          | 47      | 13 | 0  | 1  | 1  | 38 |    | $\sigma^*$ |
| 5.7                           | 6       | 6  | 23 | 19 | 0  | 56 |    | $\sigma^*$ |
| 1.8                           | 16      | 0  | 0  | 81 | 1  | 2  |    | $\sigma^*$ |
| <b><math>HRh_2SnRh</math></b> |         |    |    |    |    |    |    |            |
| 13.4                          | 27      | 48 | 8  | 5  | 2  | 10 |    | $\sigma$   |
| 9.5                           | 24      | 27 | 5  | 2  | 0  | 42 |    | $\sigma^*$ |
| 4.3                           | 1       | 7  | 14 | 9  | 0  | 69 |    | $\sigma^*$ |
| 0.8                           | 29      | 0  | 55 | 9  | 1  | 6  |    | $\sigma^*$ |
| level<br>$-\epsilon$ , eV     | H<br>1s | Zn |    |    | Rh |    |    | nature     |
|                               |         | 4s | 4p | 3d | 5s | 5p | 4d |            |
| <b><math>HRh_3Zn</math></b>   |         |    |    |    |    |    |    |            |
| 10.1                          | 47      | 0  | 0  | 0  | 21 | 9  | 23 | $\sigma$   |
| 6.1                           | 7       | 20 | 0  | 1  | 0  | 0  | 72 | $\sigma^*$ |
| 4.1                           | 9       | 37 | 6  | 0  | 20 | 0  | 28 | $\sigma^*$ |
| 1.7                           | 10      | 1  | 0  | 0  | 45 | 39 | 5  | $\sigma^*$ |
| <b><math>HRh_2ZnRh</math></b> |         |    |    |    |    |    |    |            |
| 12.2                          | 10      | 5  | 3  | 82 | 0  | 0  | 0  | $\sigma$   |
| 10.3                          | 33      | 10 | 4  | 14 | 23 | 6  | 10 | $\sigma$   |
| 7.3                           | 4       | 12 | 0  | 0  | 17 | 4  | 63 | $\sigma^*$ |
| 3.4                           | 12      | 1  | 11 | 0  | 16 | 15 | 45 | $\sigma^*$ |
| <b><math>HZn_4</math></b>     |         |    |    |    |    |    |    |            |
| 12.9                          | 12      | 20 | 13 | 55 |    |    |    | $\sigma$   |
| 10.7                          | 15      | 48 | 3  | 34 |    |    |    | $\sigma$   |
| 7.2                           | 20      | 66 | 14 | 0  |    |    |    | $\sigma^*$ |
| 3.8                           | 15      | 64 | 18 | 1  |    |    |    | $\sigma^*$ |

nearly the same energy as the antibonding level of  $HSn_4$ . In the bimetallic systems these two levels mix, yielding the Sn-H antibonding level discussed above. On the other hand, the bonding level of  $Sn_4$  is stabilized by the interaction with hydrogen. We conclude that the replacement of a Pd atom with Sn gives rise to  $\sigma$  and  $\sigma^*$  levels between the bimetallic surface and the hydrogen. The antibonding level is now in competition with the bonding level

Table IV. Net Atomic Populations<sup>a</sup>

| cluster                               | bare cluster |       | with hydrogen |       |      |
|---------------------------------------|--------------|-------|---------------|-------|------|
|                                       | Pd           | Sn    | Pd            | Sn    | H    |
| Pd <sub>3</sub> Pd (3,1)              | 16.00        |       | 15.94         |       | 1.28 |
| Pd <sub>3</sub> Sn (3,1)              | 16.09        | 3.75  | 15.99         | 3.72  | 1.30 |
| Pd <sub>2</sub> SnPd (3,1)            | 16.07        | 3.79  | 15.99         | 3.78  | 1.23 |
| Sn <sub>3</sub> Sn (3,1) <sup>b</sup> |              | 4.00  |               | 3.97  | 1.12 |
|                                       | Rh           | Sn    | Rh            | Sn    | H    |
| Rh <sub>3</sub> Rh (3,1)              | 15.00        |       | 14.91         |       | 1.35 |
| Rh <sub>3</sub> Sn (3,1)              | 14.98        | 4.06  | 14.85         | 4.11  | 1.34 |
| Rh <sub>2</sub> SnRh (3,1)            | 15.01        | 3.97  | 14.97         | 3.93  | 1.18 |
| Sn <sub>3</sub> Sn (3,1) <sup>c</sup> |              | 4.00  |               | 3.97  | 1.12 |
|                                       | Rh           | Zn    | Rh            | Zn    | H    |
| Rh <sub>3</sub> Zn (3,1)              | 15.07        | 11.78 | 15.12         | 11.56 | 1.07 |
| Rh <sub>2</sub> ZnRh (3,1)            | 15.07        | 11.77 | 15.02         | 11.97 | 1.14 |
| Zn <sub>3</sub> Zn (3,1) <sup>c</sup> |              | 12.00 |               | 11.95 | 1.22 |

<sup>a</sup>The given values are the average population for the atoms.

<sup>b</sup>Lattice parameter of Pd. <sup>c</sup>Lattice parameter for Rh.

observed in the HPd<sub>4</sub> interaction. Similar analyses can be performed for the energy levels of the RhSn alloys. The eigenvector compositions reported in Table III show strong similarities to their PdSn analogues.

As mentioned before, in the case of Zn-containing clusters, replacement in the second layer does not lead to a decrease in the hydrogen interaction energy but rather to an increase. The reason for this is not transparent; however, looking at Figure 3 and Table III we can see that the interactions are in some important respects different from those just discussed for Sn. The details depend on the position of the Zn atom in the cluster. Comparing HRh<sub>3</sub>Zn first with Rh<sub>4</sub> and then with HRh<sub>3</sub>Sn, we note that the main split-off state (47% H is in all cases) involves no contribution from the Zn; the main effect of alloying on this level is that the Rh atoms have a somewhat different hybridization, being slightly less rich in d electrons and correspondingly more rich in p. In the Sn alloy there is a significant Sn(s) contribution in this level and the Rh's have almost exclusively d character. Differences in the  $\sigma^*$  levels also exist, but we see no simple use of these to rationalize the increased binding energy. When Zn is in the first layer, HRh<sub>2</sub>ZnRh, then one immediately apparent aspect is that the Zn d functions are involved in the split-off states at -12.2 and -10.3 eV. This added complexity may be both a boon and a bane; it complicates the description of the bonding but may also provide added variability in catalyst "optimization". It will be very interesting to see how such alloys perform in practice.

In Table IV are collected the net atomic charges for all the M<sub>4</sub> clusters without and in the presence of hydrogen. For the bare clusters the effect of the non-transition metal replacement is, with the exception of Rh<sub>3</sub>Sn, a slight electron surplus on the transition-metal atoms, in line with the relevant electronegativities (Pauling values of 2.28 (Rh), 2.20 (Pd), 1.96 (Sn), and 1.65 (Zn)). The addition of H causes a charge transfer, and the electron surplus on hydrogen comes more from the transition metal than the non-transition metals. The position of tin has the same consequences in both Pd and Rh. The case with zinc in the second layer shows the lowest charge transfer, and this should be related to the observed increased hydrogen binding energy.

**Hydrogen Diffusion on and in Pure and Bimetallic Clusters and Implications for Catalysis.** Returning to the high-*T* thermodesorption peak,<sup>6c,e</sup> we were prompted to shift from questions of bond strength (thermodynamics) to those of dynamics by the realization that the presence of the high-*T* peak depends on the catalyst's history; it is present only if chemisorption has taken place at high temperature. We have therefore calculated the barriers for diffusion both into the bulk and along a (100) surface for the pure transition metals and in the presence of Sn, the idea being that H atoms (from H<sub>2</sub> previously dissociated on (nearly) pure transition-metal regions of the catalysts) could perhaps be driven across the higher diffusion barriers in the presence of Sn and trapped when the temperature is lowered. It would then require a high

Table V. Calculated Energy Variations for Hydrogen Diffusion in the Bulk of Different Pd and PdSn Clusters<sup>a</sup>

| cluster                                    | a/eV | b/eV | c/eV |
|--|------|------|------|
| Pd <sub>10</sub> (3,3,1,3)                 | 0.79 | 0.39 | 0.40 |
| Pd <sub>13</sub> (6,6,1)                   | 0.78 | 0.45 | 0.33 |
| Pd <sub>16</sub> (6,6,1,3) <sup>b</sup>    | 0.87 | 0.63 | 0.24 |
| Pd <sub>6</sub> Sn <sub>6</sub> Pd (6,6,1) | 1.15 | 0.60 | 0.55 |
| exp <sup>b</sup>                           |      |      | 0.26 |

<sup>a</sup>For the definitions of *a*, *b*, and *c* parameters see Figure 5. <sup>b</sup>Not corrected for BSSE. <sup>c</sup>From ref 18a.

temperature to make them diffuse, meet a partner H atom, and desorb as H<sub>2</sub>. Indeed, it turns out to be the case that diffusion barriers into the bulk (HPd<sub>13</sub> vs HPd<sub>7</sub>Sn<sub>6</sub>) and over a (100) surface (HPd<sub>8</sub> vs HPd<sub>6</sub>Sn<sub>2</sub> and HRh<sub>3</sub>Sn<sub>3</sub>) are increased in the presence of tin.

We emphasize again that the calculated barriers correspond to a lattice frozen at the experimental bulk geometry of the pure transition metal. Lattice dynamics would likely lower these<sup>15</sup> whereas relaxation from the transition-metal structure to that of the alloy (probably a shrinking, due to the smaller size of Sn) might increase them, at least for penetration into the bulk. Other sources of uncertainty include cluster size effects and the inherent inaccuracies of the LDF method (unfortunately, there has not yet been much systematic study of transition states and barriers with local or nonlocal functionals). Nevertheless, the trend is so clear (proximity of H to Sn always leads to a strong destabilization) that we accept it as the basis for the following analysis.

Although the high-*T* thermodesorption peak was observed for RhSn catalysts, for the case of diffusion into the bulk we have studied the PdSn alloys. There are two reasons for this: First, experimental information about diffusion is more prevalent for Pd<sup>9,18a,26,27</sup> and comparisons with our calculations are then possible. Second, we are interested in the magnitude of the effects of tin substitution on the dynamics. Because we have found that the perturbation to the binding is similar for small Pd and Rh clusters, and since pushing a system across a diffusion barrier represents a rather small change to the electronic structure, it is likely that the general features calculated for one of the metals will also be valid for the other. In fact, we will see that the whole set of results is "self-consistent". Previous calculations on pure rhodium have shown that the general shapes of the potential energy curves are similar to those for palladium, the barriers being scaled upwards. For the simulation of hydrogen diffusing through a (111) surface we have used a number of different clusters. The results are collected in Table V. Considering that the results for Pd<sub>16</sub> are not corrected for the (undoubtedly small) BSSE, all the results on pure Pd clusters are consistent and, apparently, converged with respect to cluster size. (The results for Pd<sub>10</sub> are slightly different from those reported in ref 25a. In fact we are unable to reproduce the earlier results exactly. The present results have been reproduced by several workers and their internal consistency likely means that the earlier results suffered from a (numerically small) error. None of the conclusions of ref 25a are significantly changed by this.) The octahedral site (see Figure 5) is found to be 0.3–0.4 eV less stable than the chemisorption minimum. The experimental counterpart is 0.26 eV.<sup>18a</sup> The maximum is found when the hydrogen lies at the center of the three palladium surface atoms (TRI of Figure 5). The barrier for diffusion is about 0.8 eV for all the clusters considered. The effect of adding a non-transition metal has been simulated by replacing six Pd atoms of the first and second layers by Sn (Figure 1). This corresponds to a situation of indirect interaction. In this arrangement the energy of the octahedral site rises to 0.55 eV above the chemisorption minimum and the barrier for entrance into the bulk is increased to 1.15 eV. For purposes of comparison, in Figure 5 the potential curves for both Pd<sub>13</sub> and Pd<sub>7</sub>Sn<sub>6</sub> are shown. We can conclude that the presence of Sn has a distinct effect on the diffusion barriers and this could be offered as an explanation of the high-*T* thermodesorption peak, the hydrogen being driven into the bulk during the cooling from high temperature and trapped there at lower temperature, only to be released when the temperature is raised again.

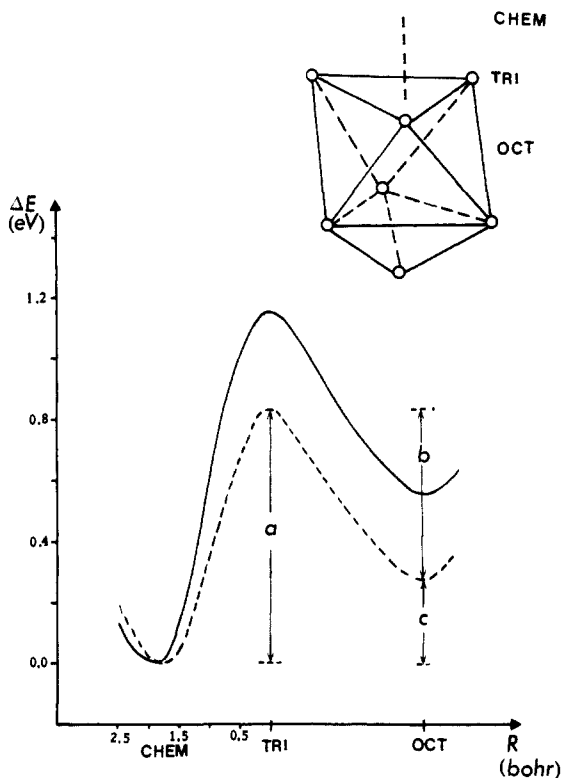


**Figure 5.** Relative energy of hydrogen at various positions with respect to a 13-atom cluster (the inset defines the sites and shows only the central part of the cluster): (---) (HPd<sub>13</sub>), (—) (HPd<sub>7</sub>Sn<sub>6</sub>) (see Figure 1 for positions of metal atoms).

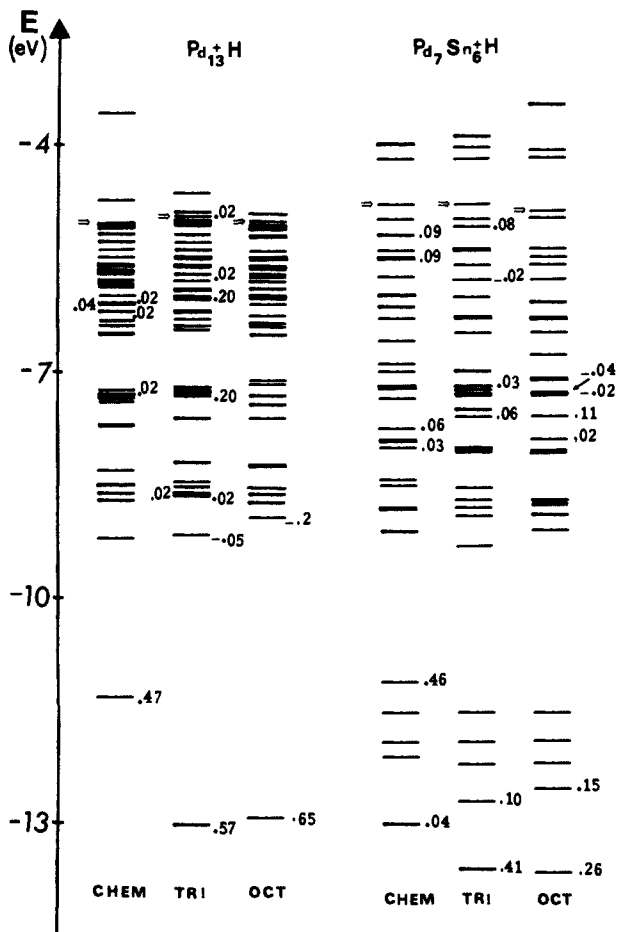


**Figure 6.** Orbital energies for a hydrogen atom at various sites with respect to a 13-atom cluster: (A) HPd<sub>13</sub>, (B) H-Pd<sub>7</sub>Sn<sub>6</sub>. See inset to Figure 5 for the definition of sites.

**Table VI.** Calculated Parameters for the Hydrogen Surface Diffusion on a Rh<sub>8</sub>Sn<sub>3</sub> Cluster<sup>a</sup>

| position | site   | $R_{\perp}/\text{\AA}$ | $R_{\parallel}/\text{\AA}$ | $\omega_e/\text{cm}^{-1}$ | $\Delta E/\text{eV}$ |
|----------|--------|------------------------|----------------------------|---------------------------|----------------------|
| 1        | 4-fold | 0.23                   | 1.92                       | 777                       | 0.00                 |
| 2        | bridge | 1.07                   | 1.72                       | 1760                      | 0.26                 |
| 3        | 4-fold | 0.89                   | 2.10                       | 882                       | 1.31                 |
| 4        | bridge | 1.33                   | 1.89                       | 1140                      | 1.42                 |
| 5        | 4-fold | 0.76                   | 2.05                       | 877                       | 1.15                 |

<sup>a</sup> For the definition of positions and structure of the cluster see Figure 7.

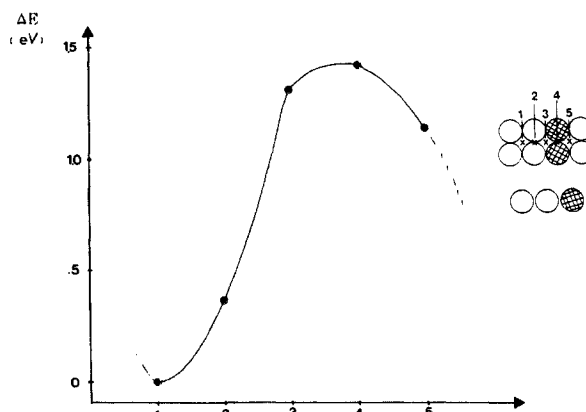


**Figure 7.** Relative energy of a hydrogen atom at various positions on a Rh<sub>8</sub>Sn<sub>3</sub> cluster. The inset shows the positions of the Rh (open circles) and Sn (cross hatched circles) atoms and defines the sites. For each site the height above the surface was optimized.

We will soon see that other explanations can also be offered.

To complete the discussion for bulk diffusion, we show in Figure 6 the orbital energy diagrams of HPd<sub>13</sub> and HPd<sub>7</sub>Sn<sub>6</sub> for the two minima (CHEM and OCT of Figure 5) and at the maximum of the considered pathway. The hydrogen character, as judged by a Mulliken analysis, is indicated wherever it is greater than 2%. The most obvious feature of the diagram is the split-off state<sup>18,25,28</sup> near -11.5 eV (for HPd<sub>13</sub> and at somewhat lower energies for the other two sites). The presence of tin increases the number of states in this region, as expected. For the chemisorption case the split-off state is relatively unperturbed. However, for the TRI and OCT positions which are in closer proximity to the Sn atoms a second level with quite significant hydrogen population can be identified. These are the analogues of the Sn-H antibonding levels discussed in the last section and are responsible for the increased barrier.

We next turned our attention to diffusion, not into the bulk but over the surface of the clusters. This was motivated by the idea that the high-*T* thermodesorption peak corresponded to hydrogen that was activated for the catalytic process. In fact there is a good correlation, perhaps coincidentally, between the reactivity of a given catalyst for ester hydrogenation and the amount of hydrogen desorbed at high temperature in the TPD experiment. In any event we will see that surface diffusion barriers might also play a role in explaining the thermodesorption and aspects of the catalysis.

The surface diffusion has been studied for both Pd and Rh clusters including some Sn substitutions, HPd<sub>8</sub> vs HPd<sub>6</sub>Sn<sub>2</sub> and HRh<sub>8</sub>Sn<sub>3</sub>. Since the conclusions are similar and since the rhodium study involves a single cluster for all of the considered sites whereas the palladium study does not, we report only the rhodium results. The energies are given in Table VI, and the energy profile along with the definition of the cluster sites is shown in Figure 7. The tendency found for the binding energies and for diffusion into the bulk is continued here—putting H near Sn is less favorable energetically than putting it near Pd or Rh. In particular, from Table VI and Figure 7, it is clear that the binding energies decrease on going to sites where the presence of tin is more pronounced, either in number or by proximity. We emphasize that this is a general



result for all the cases we have studied and should transcend our particular choices of model. We have not examined all possible diffusion paths but we believe that the principle is well established that diffusion paths leading to proximity of the hydrogen to tin are energetically costly. Indeed, if one considers that the binding energy of gas-phase  $H_2$  is about 2.4 eV per atom and that the binding energy of H to a pure Rh cluster of this size should be between 3.5 and 4 eV then the barriers shown in Figure 7 for sites close to Sn would bring the system quite close to the desorption limit (for  $H_2$  desorption) so that the order of magnitude is right to consider the possibility that surface diffusion could be rate limiting. Clearly experimental study of the surface diffusion on well-defined alloy surfaces (such as those performed by Paffett et al.<sup>29</sup>) would be of great interest.

Hence, a possible explanation for the high- $T$  thermodesorption peak, in which the H atoms are held on the surface for reasons of the kinetics of surface diffusion rather than for thermodynamical reasons, emerges from the calculations. We hasten to add that an alternative explanation of the TPD has been proposed<sup>6c</sup> involving surface hydroxyl groups or water on the support, which produce  $H_2$  following the oxidation of tin. Further work will be required to see if this proposal or the one just described will prevail. In either event, the diffusion calculations have brought to light the possibility of the importance of diffusion rates in the sense just described, an importance beyond "mere" mass transport.

Indeed, one can imagine a scenario for catalysis in which the very existence of an activated species is owed to the lower mobility associated with high surface diffusion barriers. In the present case "activated" H (remember, the binding energy is lowered in Sn-rich areas) is held on the surface (ready to react?) because it cannot diffuse rapidly to meet another H atom and desorb. It will be interesting to see if other such cases can be discovered through further calculations and through experiments.

### Conclusions

On the basis of our work we can draw some conclusions that we believe shed light on the way hydrogen interacts with bimetallic catalysts both in a "static" and in a "dynamic" sense. We also think they should prove useful in guiding interpretations of the catalytic properties of these materials. First we stress that in all cases where direct comparisons with experiment are possible, they

are favorable. The basic LCGTO-MCP-LSD approach is up to the task of describing the type of interactions studied. The cluster models have been chosen to represent a wide variety of adsorption sites so that some generality can be claimed. The first result we emphasize is the decrease of the hydrogen binding energy due to the presence of tin. This decrease has been found in the case of both direct and indirect Sn-H interactions, and both "geometric" and electronic effects participate. The change in binding energy has been traced to the occupation (or lack of emptying) of orbitals with Pd-H or Rh-H bonding interactions but of Sn-H antibonding character. The effect appears to operate (binding energy changes of a few tenths of an eV) out to second-neighbor distances. For RhZn alloys, one case of a binding energy increase has been uncovered. It has also been found that for Zn atoms next to adsorbed hydrogen, the d electrons interact with H 1s to a significant extent. It will be interesting to see how such alloying affects the chemisorption energies of other, more complex, adsorbates (reactants, products, "undesirable" carbonaceous material, etc.). The decreased stability of hydrogen in the proximity of tin also manifests itself in the increased barriers to diffusion into the bulk or along the surfaces of the alloys. This has been offered as a plausible explanation for the high-temperature thermal desorption peak observed for Rh-Sn alloys following adsorption at high  $T$ . It has also been proposed that the higher diffusion barriers might play a novel role in catalysis by preventing activated hydrogen from meeting a partner H atom to form  $H_2$  and desorb. This aspect underlines the obvious, but often overlooked, fact that reactions depend not only on energetics but also on kinetics and on dynamics, more generally. If nothing else, we feel our calculations will have served a useful purpose if this reminder helps to keep this point in mind for future theoretical and experimental studies.

**Acknowledgment.** We are grateful to the Natural Sciences and Engineering Research Council of Canada, to the Fonds FCAR of Quebec, to the Institut Français du Pétrole, to the Società INTERSEIL (Rende), CNR (Italy), and to NATO for financial support and to the Centre de Calcul de l'Université de Montréal, NSERC's Supercomputing Program (access to the Cray-1 and XMP at the Atmospheric and Environmental Services—Canada and the Cray-XMP at the Ontario Centre for Large Scale Computation) and to Cray Canada for providing computing resources. Peter Fillmore's (Cray Canada) interest and support are most appreciated. We appreciated stimulating discussions with F. Raatz, J. P. Bournonville, G. Mabilon, and J.-P. Candy.

(29) (a) Paffett, M. T.; Gebhard, S. C.; Windham, R. G.; Koel, B. E. *Surf. Sci.* **1989**, *223*, 449. (b) Paffett, M. T.; Gebhard, S. C.; Windham, R. G.; Koel, B. E. *J. Phys. Chem.* In press.